



VIBRATION ANALYSIS OF A TWIN-SCREW COMPRESSOR AS A POTENTIAL SOURCE FOR PIEZOELECTRIC ENERGY HARVESTING

CLAUDIA SĂVESCU^{1,2}, VALENTIN PETRESCU^{1,2}, DANIEL COMEAGĂ², IULIAN VLĂDUCĂ¹,
CRISTIAN NECHIFOR^{1,2}, FILIP NICULESCU¹

Keywords: Energy harvesting; Vibration analysis; Twin-screw compressor, Piezoelectric harvester; Resonant frequency.

The paper presents the vibration spectra of a twin-screw compressor driven at various functioning regimes. The tests are performed to assess the potential of this rotary bladed machine as energy harvesting source. It is sought to determine the optimum spots on the compressor skid where piezoelectric harvesters can be placed, meeting the operational conditions. Like most of the industrial machinery, compressors exhibit inherent vibrations and heating during operation. The pulsatory effects of the compressed air trapped between the compressor's male and female rotors inside the compressor also give birth to harmonics. It is important to evaluate the temperatures as well since piezoelectric harvesters should preferably operate close to room temperature so as not to deteriorate the material and avoid thermal hysteresis, which can ultimately lead to the loss of piezoelectric properties. The study herein involves acquiring vibrational data and representing it graphically as vibration spectra. An analytical model is also presented for calculating the main frequencies of the compressor, validated by the experimental data measurements. We also present laboratory tests with the piezoelectric harvester tuned near the male rotor's frequency for achieving resonance conditions. The male rotor frequency was the most stable, with the highest amplitudes and of convenient value (~83 Hz) for the tip mass required for decreasing the piezoelectric cantilever's resonant frequency from ~210 Hz.

1. INTRODUCTION

Microenergy harvesting is an engineering direction that has begun to gain an increased interest in the last two decades and is being thoroughly researched at the present moment [1]. Many research papers deal with vibration and noise study and analysis [2], without exploiting it. Other papers aim to increase the power output in laboratory conditions or address structural changes to the harvesters in FEM (Finite Element Method) simulations. However, only some scientific articles in the literature address the source's potential [3-6]. Dealing with piezoelectric harvesters (PEH), especially their need to operate at resonance frequency, may be easy to achieve in laboratory setups. Still, it is a whole different story in conditions resembling in-situ operation. Furthermore, the application sought is part of a multisource energy harvesting system with thermoelectric generators (TEG), which require a thermal gradient to produce energy.

Harnessing energy from industrial machinery available on test benches [7-10] offers the challenge of a comprehensive view of the vibration levels and temperature ranges and, thus of the electric output to be expected from the harvesters. Harvesting from multiple energy sources on the same equipment is quite challenging, especially when using piezoelectric resonant structures and thermoelectric generators, which are generally incompatible [11].

Piezoelectric devices have a high energy conversion efficiency. However, this happens only at resonance. Before placing the piezoelectric resonant structure on the compressor, this one's natural frequency must be adjusted to match the frequency of the compressor. Outside resonance, the electric response of a cantilever beam with a seismic tip mass is very poor. Harvesting vibration energy mainly aims to eliminate cabling in the sites with difficult conditions or space constraints. A possible application would be powering sensor nodes in hazardous locations [12], where regulations are applied for using costly explosion-proof certified equipment and cabling in the

field, subjected to the ATEX Directive in Europe.

Resonant piezoelectric structures must achieve resonance conditions at a bending mode (usually fundamental frequency, first bending mode) [1]. Piezoelectricity is successfully used for actuation and sensing, and the technology for energy generation is recording an increasing interest for research, development, and optimization, as proven by the numerous papers in the literature. Nevertheless, it still has a long way to go until it reaches a satisfying technological maturity regarding stability over energy source variations and electric energy converted and supplied to the load.

Few research papers address a real source to harvest vibration from [3-5], the vast majority only focusing on obtaining maximum output by exciting the structures at their natural frequencies within simulations or laboratory tests. In this competitive urge to get even a slightly improved electric response, using more or less "orthodox" methods or simulating complicated designs that could not be feasible in real, many researchers have forgotten what this micro energy harvesting technique was promising when it emerged. The ultimate aim was powering wireless sensor nodes and recharging a battery for structural health monitoring of machinery. In industrial in-situ operation [13,14], it is not possible to drive the machinery to match harvesters' natural frequencies, as the purpose of those machines with inherent vibrations is not to work as shaker tables. Still, on the contrary, the desire is to minimize the vibration.

This work moves toward the goal and proposes a realistic approach to harvesting vibration energy from an industrial twin-screw compressor [15-19] on a test bench.

2. OVERVIEW OF COMPRESSOR UNIT AND SKID

A twin-screw compressor, whose cutaway 3D model is presented in Fig. 1, is a positive displacement compressor (volumetric), classified as a rotary-bladed machine. The

¹ Romanian Research and Development Institute for Gas Turbines COMOTI. Corresponding author, E-mail: claudia.borzea@comoti.ro, valentin.petrescu@comoti.ro; iulian.vladuca@comoti.ro; cristian.nechifor@comoti.ro; filip.niculescu@comoti.ro.

² University Politehnica of Bucharest. daniel.comeaga@upb.ro.

purpose of the use is to elevate gas or air pressure in applications requiring it, such as gas extraction and transportation, testing pneumatic equipment, *etc.*

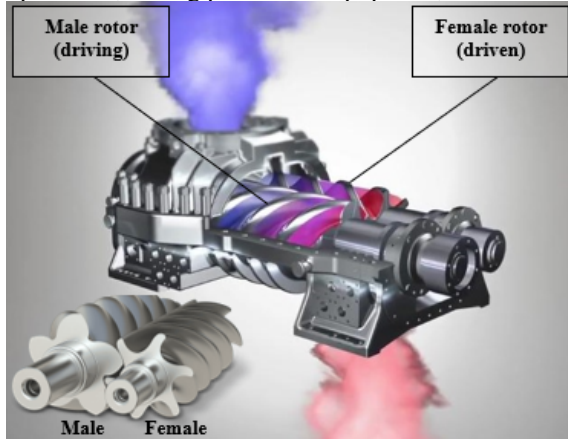


Fig. 1 – Twin-screw compressor cutaway and rotor profile (from [20]).

A rotary screw compressor [21] achieves gas compression by employing a set of male and female helically grooved rotors [22], designed in such a way as to gradually reduce the space between them from the inlet towards the outlet. Hence, the gas volume inside the compressor unit is trapped between the intermeshing rotors and the housing, reducing the gas volume progressively (Fig. 2). The volume reduction results in gas compression.

Natural gas compressors are tested before commissioning with air as working fluid regarding vibration levels, pressure, power, and temperature. Testing with gas would require infrastructure and anti-explosion certifications for gas supply pipelines, also adding to these the high additional costs for gas. The tests aim to detect inchoate faults such as shaft misalignments, poor screws tightening, and potential gripping of the rotors and to test the lubrication installation to avoid friction between the rotors.

The vibration measurements were carried out on the compressor skid presented in Fig. 2, outlining its main components. The compressor normally works in a quasi-stationary regime without speed variation during operation.

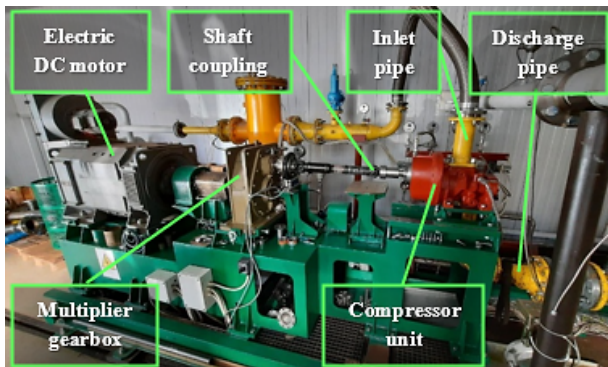


Fig. 2 – Compressor skid on the test bench (from [3]).

3. ANALYTICAL MODEL FOR COMPRESSOR VIBRATION FREQUENCIES

Vibrations are usually caused by unbalances, shaft misalignments, loosened screws, bearing issues, or resonances at critical speeds. The discharge pulsation levels downstream of the compressor are directly controlled by the difference between the compressor's internal pressure and the pressure in the discharge pipe.

The discharge pulsations are minimized when the internal pressure equals the discharge line pressure. Pulsations ought to be avoided, and they are attenuated using a separator vessel, which plays a damper (attenuator) role in the case of our installation. Generally, the harvested vibrations are the non-dangerous ones from the rotational speeds discussed.

Screw compressors produce pulsations during operation [23], leading to vibration and noise in the upstream and downstream piping systems. The frequencies are strongly related to the mechanism that produces the pulsations. The compressor frequency depends on compressor speed and on the number of rotor lobes. The CU90G compressor is designed with $z_{male} = 5$ lobes for the male rotor and female rotor with $z_{female} = 6$ lobes. The frequency of the working process, also known as pocket passing frequency, is calculated by male rotor frequency multiplied by the number of male rotor lobes:

$$f_f = f_{male} \cdot M_{lobes} , \quad (1)$$

where: f_f [Hz] – fundamental frequency; f_{male} [rpm] – male rotor frequency; M_{lobes} [ND] – male rotor lobes.

The speed of the male rotor is determined by multiplying the electric motor's speed with the gearbox's multiplication factor i . In our case, $i = 2.032$.

$$n_{male} = n_D \cdot i , \quad (2)$$

where: n_{male} [rpm] – male rotor speed; n_D [rpm] – driver (motor) speed; i [ND] – gearbox multiplication factor.

Besides the main fundamental frequency, the compressor also exhibits vibrational frequencies caused by the two rotors' rotational speeds, given by relations (3) and (4) [15]:

$$f_{male} = n_{male}/60 , \quad (3)$$

$$f_{female} = f_{male} \cdot z_{male}/z_{female} , \quad (4)$$

where: f_{male} [Hz] – male rotor frequency; n_{male} [rpm] – male rotor rotational speed; f_{female} [Hz] – female rotor frequency; z_{male} [ND] – number of lobes of the male rotor; z_{female} [ND] – number of lobes of the female rotor.

The maximum vibration amplitudes occur due to the relative rotational resonance between male and female rotors. The vibration magnitude increases proportionally with the operating speed for the discharge pressure pulsations, given by the internal volume ratio of the compressor, which is related to the internal pressure ratio according to:

$$P_i = V_i^k , \quad (5)$$

where: P_i [ND] – internal pressure ratio; V_i [ND] – internal volume ratio; k – specific heat ratio of the compressed gas ($k = c_p/c_v$ for ideal gases, typically $k \cong 1.3$).

Table 1

Frequencies given by the number of lobes and rotors' rotational speeds

No.	n_D [rpm]	n_{male} [rpm]	f_{male} [Hz]	f_{female} [Hz]	f_f [Hz]
1	1000	2032	33.86	24.14	169.3
2	1500	3048	50.8	36.3	254
3	2000	4064	67.7	48.35	338
4	2500	5080	84.7	60.5	423
5	3000	6096	101.6	72.57	508

Pressure bursts and pressure differences of trapped gas volumes also give birth to shocks along the longitudinal shaft axis. This transient pulsatory behavior due to the air

compression process is the cause of the higher-order harmonics. The harvested vibrations are preferred to be the non-dangerous ones, and the piezoelectric resonant structures can be easily adjusted to the compressor's operating frequencies, preferably with good enough amplitudes and accelerations.

Table 1 presents the calculated values of the compressor fundamental frequency, f_b , given by the pocket passing frequency, and of the frequencies given by the rotational speeds of male and female shafts for different driver speeds.

4. VIBRATION MEASUREMENTS AND ACQUIRED DATA ANALYSIS

The measurements were carried out on the compressor unit using an industrial vibration analyzer with a triaxial piezoelectric accelerometer as the sensing element. For vibration measurement, the compressor's speed was varied via the frequency converter controlling the dc driving motor's speed. The section of the discharge motor-operated valve (MOV) is controlled and reduced gradually to create a pressure of 6 bar and 9 bar, respectively, for the conducted measurements. Five points on the compressor housing, where the vibrations are known to be higher (Fig. 3), and four-speed stages were considered, namely: **1)** 1000 rpm; **2)** 1500 rpm; **3)** 2000 rpm; **4)** 2500 rpm.

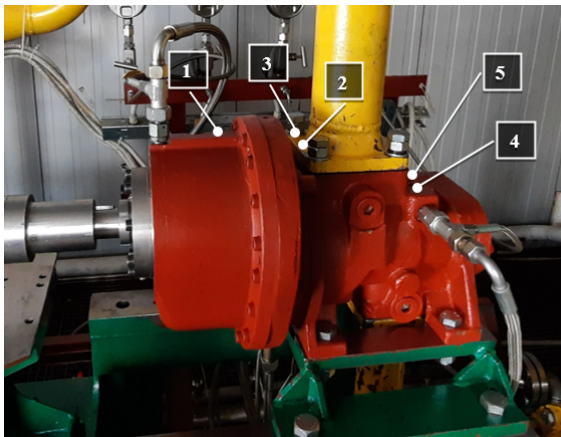


Fig. 3 – Measuring points considered.

The longitudinal axis of the accelerometer, Y, is oriented along the compressor shaft's axis, Z is the vertical axis, and X is the transverse axis concerning the shaft (see Fig. 4).

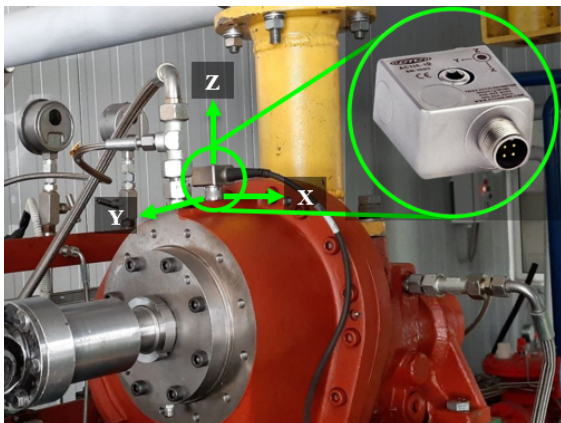


Fig. 4 – Triaxial accelerometer in point 1 and axes orientation.

A thermographic image with markers in points where vibrations were measured is presented in Fig. 5. The temperature needs to be known before placing any

piezoelectric devices, as these exhibit a significant thermal hysteresis and high temperatures are prone to cause thermal aging [24] and loss of piezoelectric properties. The lead zirconate titanate (PZT-5H) piezoelectric material of our harvesters should preferably be installed and kept around room temperature, $20 \div 25 \text{ }^\circ\text{C} \pm 10 \text{ }^\circ\text{C}$ [25]. As one can observe in the thermographic image, points 4 and 5 exhibit higher temperatures closer to the exhaust port, more precisely at the end section between the rotors, where high pressures and, consequently, high temperatures are met. Even though point 2 seems to be thermally optimal, points 2 and 3 have a spatial constraint that does not allow fitting in the PEH with its support for preliminary testing. A hot point marker is also displayed near the exhaust, at $64.5 \text{ }^\circ\text{C}$.

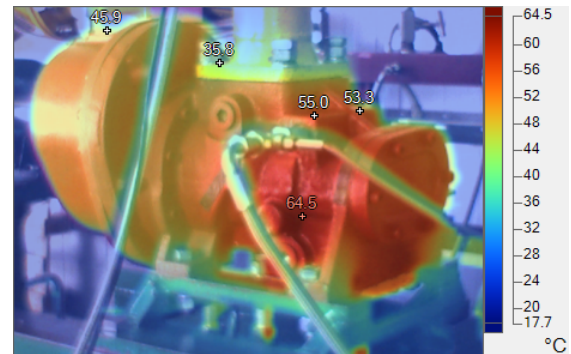


Fig. 5 – Thermographic image of the compressor unit.

The measured vibration data was recorded and saved for subsequent post-processing and analysis. After applying the FFT-embedded function, the frequency spectra are presented in the plots. The data acquisition was conducted with a 0.5 Hz frequency resolution.

Figure 6 shows the vibration speed magnitude function of frequency in point 1 at a running speed of 2500 rpm and developing a pressure of 6 bar at compressor discharge. The frequency components are caused by the multiple parts in motion, such as the male rotor (83.5 Hz) and the female rotor (41.5 Hz). The compressor's fundamental frequency (first harmonic) is 423.5 Hz. From the spectrum below, a second-order harmonic can also be noticed (847 Hz).

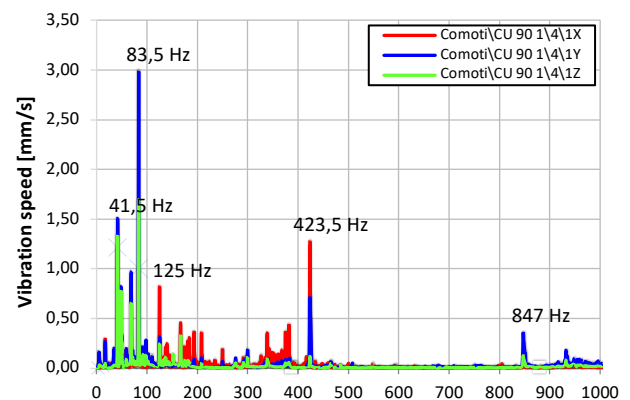


Fig. 6 – Frequency spectra in point 1 at 2500 rpm and 6 bar.

The data from all the measuring points has been plotted as 3D ribbon graphs in LabView to have a more comprehensive overview of the vibrations measured and which point would be optimal. In Fig. 7, we plotted the vibration spectra in the vertical Z direction in all five points. Point 1 is the most convenient regarding amplitudes.

In Fig. 8, we plotted the vibration spectra, compiling the measured data in the Y direction (along the compressor shaft) in all five points. As one can notice, in point 1, the vibration amplitudes are almost double that in the vertical direction.

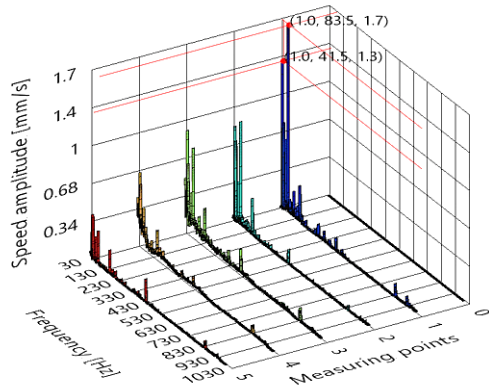


Fig. 7 – 3D plot showing the vibration spectra on Z axis for all points.

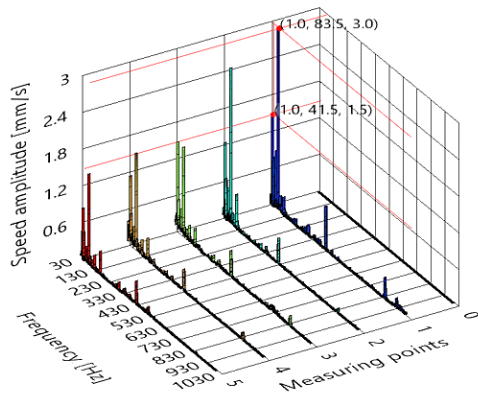


Fig. 8 – 3D plot showing the vibration spectra on Y axis for all points.

4. LABORATORY TESTS WITH PIEZOELECTRIC HARVESTER WITH TUNED FREQUENCY

The laboratory setup, with its main components, is presented in Fig. 9. The equipment used is specific to laboratory setups used for piezoelectric devices [26,27], consisting of an electrodynamic shaker table, accelerometer, dynamic spectrum analyzer with embedded functions generator, power amplifier, and piezoelectric harvesting system to be tested, placed on the shaker.



Fig. 9 – Experimental setup.

The experimental setup employs the following main equipment:

- **SR785 spectrum analyzer** with functions generator and automatic FFT (Fast Fourier Transform);

- **TIRA S 513 shaker table**, driven by the analyzer with a swept-sine signal amplified via the power amplifier;
- **TIRA BAA 120 power amplifier**, with sinusoidal output power (120 VA RMS);
- **Piezoelectric energy harvesting system (Midé PPA-4011 + Midé PPA-9001 clamp kit [28])**, attached on the shaker with double-sided adhesive tape;
- **A Brüel&Kjær 4508-001 accelerometer**, used as reference input signal for vibration amplitude. The sensitivity of this accelerometer is 1 mV/m/s^2 .

A stepping swept-sine signal is employed, generated by the signal analyzer to drive the shaker, which ensures a time-harmonic motion of the mechanical vibrations. This is verified by the accelerometer placed on the shaker's mobile platform or the harvester's support. The accelerometer connects to input channel 1, and the piezoelectric harvester connects to input channel 2. The output of the spectrum analyzer is connected to drive the shaker table.

Midé PPA-4011 [28] multilayer piezoelectric harvester is a quadmorph cantilever beam with four piezoceramic wafers of lead zirconate titanate, PZT-5H. The beam has 17 very thin layers, including, besides the four piezoelectric layers, the eight copper electrodes (two for each piezo wafer), and five FR4 glass-reinforced epoxy for the electrical isolation of the copper electrodes. The structure's dimensions are $71.0 \times 25.4 \times 1.32 \text{ mm}$.

An inertial mass of 7.8 g was mounted on the cantilever tip (Fig. 10), for tuning the resonant frequency [29] of the PEH as close as possible to the male frequency of the compressor. Due to changing the mounting method employed on the compressor, we deemed it necessary to decrease the frequency slightly more than in our previous research [26]. Double-sided adhesive tape was used during laboratory tests, while on the compressor, we will employ a stronger magnetic mounting. This will require increasing the tip mass.

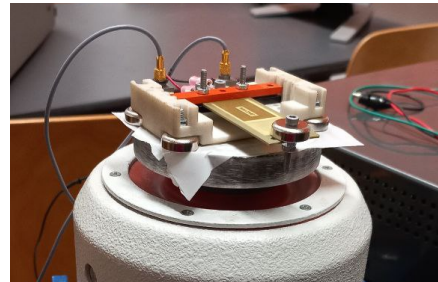


Fig. 10 – Piezoelectric harvester with tip mass on shaker table

Hence, due to increased rigidity, we are expecting a slight increase in the natural frequency of the piezoelectric harvester, which will need to be decreased by further increasing the tip mass, according to (6):

$$f_n = \frac{1}{2\pi} \sqrt{\frac{k}{m}} = \frac{1}{2\pi} \sqrt{\frac{3EI}{L^3 m}}, \quad (6)$$

where: f_n [Hz] – natural frequency; k [N/m] – bending stiffness constant; m [kg] – beam total mass; E [N/m²] – Young's modulus; I [kg·m²] – the moment of inertia of beam cross-section; L [m] – beam length.

Nonlinearities have been observed for the first time, manifesting as a double peak response around the resonant frequency. This can only be explained by material fatigue.

The data from the spectrum analyzer has been saved for subsequent processing and was plotted in Fig. 11. One can

notice that the resonant frequency is at 82 Hz, with peak voltage output of 2.81 V/g.

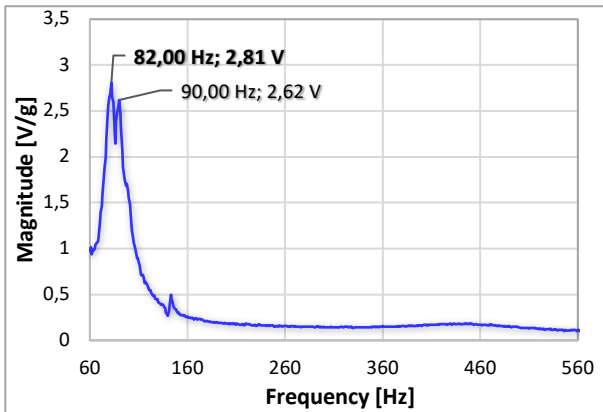


Fig. 11 – Piezoelectric voltage response vs. frequency

4. RESULTS AND DISCUSSION

The measured frequencies agree with the analytical computations (male rotor frequency measured at 83.5 Hz vs. 84.7 Hz calculated at a driver speed of 2500 rpm). The highest vibration amplitudes have been recorded along the shaft's Y direction.

It is worth mentioning that this piezoelectric cantilever, purchased in 2018, has started to lose its piezoelectric properties. The experimental tests conducted in 2018 rendered ~ 4.2 V/g with no tip mass [30]. The tests in early 2020 outlined 3.280 V/g in the same conditions with no mass [31]. We obtained a drastically decreased voltage response of 1.333 V/g with no tip mass and 5.345 V/g with a 7.4 g tip mass in our latest publication at the end of 2022 [26], which confirmed our apprehension that this piezoelectric device is getting near the end of its lifespan.

Furthermore, the results presented in the paper herein also show that we are not only dealing with the depolarization of the piezoelectric material but also with material aging and possibly micro-cracks [32]. This specific device was the most used since 2018, but we also tested the other two less-used transducers preserved in the box, exhibiting the double peak response. However, the second peak of the less used devices is lower amplitude and not pronounced. The piezoelectric harvester employed herein has also been previously installed on a gas turbine engine in 2018, which we believe to have been the starting point of material degradation due to high temperatures ($60 \div 80$ °C) [5,25].

No experimental measurements with a piezoelectric harvester can maintain the same conditions. Introducing an intermediate elastic layer on the shaker table renders an unknown and variable elasticity, further increasing due to the reuse of the double-sided adhesive tape. This alone can introduce frequency variations [34].

Table 2
Experimental results

Year	Resonant frequency f_r [Hz]	Voltage peak V_{pk} [V/g]
2018	205.25	4.205
2020	214.03	3.280
2022	208.62	1.333

During laboratory tests, the frequency of the piezoelectric transducer depends on the electrical impedance of the

spectrum analyser, $1 \text{ M}\Omega + 50 \text{ pF}$. When the PEH will be installed on the compressor, the impedance of the measuring device shall be considered. An AC-DC rectifying circuit with Schottky diodes bridges and a DC-DC converter will be required when connecting two or more piezoelectric harvesters electrically [33,34]. This complicates the problem regarding voltage drops on the electric components, as well as the accompanying frequency shifts.

It is very difficult to predict the response of the piezoelectric harvester, due to many contributing factors. Firstly, the elasticity of the double-adhesive tape is unknown and uncontrollable. Secondly, on the compressor, we will use a magnetic mount, which is a much stronger and rigid clamping. According to relation (6), the stiffness constant k is given by the clamping method, and for tuning the frequency, a tip mass will be added. The necessary mass will be established manually on the compressor by successive tries until we record an increase in the piezoelectric response, indicating that we are approaching resonance. The tests would pose quite a challenge compared to laboratory conditions, where we can sweep the frequency and find the resonance of the piezoelectric cantilever. In real applications, the machinery cannot vibrate from 60 Hz to 360 Hz and act like a shaker table.

Another issue of great concern and complexity is the thermal hysteresis, thermal aging, and the behavior of the piezoelectric device when exposed to higher working temperatures. The presented thermographic image and the decrease in the voltage output since purchase, as well as the nonlinearities in the response, hint that it has to be investigated how long piezoelectric devices can perform at best parameters on the compressor, given that the recommended room temperature ($20 \div 25$ °C) is exceeded with about 20 °C in the chosen mounting spot on the compressor, however much less than on gas turbine, with ~ 40 °C more.

The usefulness of the laboratory experiments can never be doubted for getting to know the piezoelectric device's operating parameters and behaviour, as well as observing the change in its response when introducing tip masses, electric components, modifying its working length, etc. the paper herein aims to make the first steps towards testing in relevant industrial conditions.

5. CONCLUSIONS

The paper outlines that the main spectral components of the compressor are convenient for the cantilever piezoelectric harvester. The fundamental frequency of the harvester is around 210 Hz, while the targeted frequency component to be harnessed is that of the male rotor, ~ 83 Hz. The reasons behind pursuing this specific frequency are its stability and higher amplitudes.

There are a series of limitations of the laboratory testing. First, the shaker generates vibration only in vertical direction, while the compressor exhibits vibration on all three axes. Secondly, in laboratory, the vibration frequency is swept to find the resonant frequency of the cantilever, so vibration is adjusted to match transducer's natural frequency.

In the real practical application, the harvester's frequency must be adjusted to match the compressor's. The higher temperatures on the compressor are prone to the faster material ageing and discard the use of adhesive tape and wax-mounted accelerometers, which leads to changing the mounting method to magnetic. This further implies increasing the tip mass for tuning the piezo, due to an increased stiffness than in laboratory. Hence, the real-time tuning of the piezoelectric

transducer is necessary. The thermal influences will be investigated experimentally by closely noting decreases in piezoelectric output.

Future works will study the optimal positioning and assess whether the vibration amplitude on Y (axial along the shaft) renders a better piezoelectric response than on vertical direction Z. Even though the piezoelectric devices render higher electric responses at higher vibration accelerations, it is better to excite them at lower amplitudes to prolong their lifetime.

The piezoelectric materials used in energy harvesting have yet to be studied much in the literature regarding fatigue, aging, thermal influences, and nonlinear behaviour, which are also potential future research directions.

ACKNOWLEDGEMENT

This paper was realized as part of “Nucleu” Program within the Romanian Research, Development, and Innovation Plan 2022-2027, conducted with the support of the Romanian Ministry of Research, Innovation, and Digitalization, as part of contract 31N/2023, project number PN 23.12.09.

Received on April 29, 2023

REFERENCES

1. E. W. Zhou, D. Du, Q. Cui, C. Lu, Y. Wang, Q. He, *Recent research progress in piezoelectric vibration energy harvesting technology*, *Energies*, **15**, 3, p. 947 (2022).
2. V. Anghel, C. Mareş, *Integral formulation for stability and vibration analysis of beams on elastic foundation*, *Proceedings of the Romanian Academy, Series A*, **20**, 3, pp. 285-293 (2019).
3. C. Borzea, V. Petrescu, I. Vlăducă, M. Roman, G. Badea, *Potential of twin-screw compressor as vibration source for energy harvesting applications*, *APME – Electric Machines, Materials and Drives - Present and Trends*, **17**, 1, pp. 90-95 (2021).
4. C. Borzea, D. Comeagă, A. Stoicescu, C. Nechifor, *Piezoelectric harvester performance analysis for vibrations harnessing*, *U.P.B. Scientific Bulletin, Series C Electrical Engineering and Computer Science*, **81**, 3, pp. 237-248 (2019).
5. A. Stoicescu, M. Deaconu, R. Hritcu, C. Nechifor, V. Vilag, *Vibration energy harvesting potential for turbomachinery applications*, *INCAS Bulletin*, **10**, 1, pp. 135-148 (2018).
6. C. Yang, N.B.N. Hanafi, N.B.M. Hanif, A. Ismail, H. Chang, *A novel non-intrusive vibration energy harvesting method for air conditioning compressor Unit*, *Sustainability*, **13**, 18, p. 10300 (2021).
7. M. Nitulescu, C. Slujitoru, V. Petrescu, V. Silivestru, G. Fetea, S. Tomescu, *Reducing rotors clearance – a way to increase the performance of a screw compressor*, *IOP Conference Series: Materials Science and Engineering*, **1180**, 1, p. 012007 (2021).
8. R. Catană, G. Dediu, C. Tărăbici, *Studies and experimental research in the evaluation of TV2-117A turboshaft engine working regimes*, *Applied Sciences*, **12**, 7, p. 3703 (2022).
9. A.C. Mangra, R. Carlanescu, M. Enache, F. Florean, R. Kuncser, *Numerical and experimental investigation of a micro gas turbine combustion chamber*, *International Journal of Modern Manufacturing Technologies*, **14**, 3, pp. 139-145 (2022).
10. R. Catană, G. Dediu, C. Tărăbici, H. Şerbescu, *Performance calculations of gas turbine engine components based on particular instrumentation methods*, *Applied Sciences*, **11**, 10, p. 4492 (2021).
11. D.S. Montgomery, C.A. Hewitt, D.L. Carroll, *Hybrid thermoelectric piezoelectric generator*, *Applied Physics Letters*, **108**, 26, p. 263901 (2016).
12. C. Nechifor, C. Borzea, A. Stoicescu, D. Lale, M. Vasile, *Modular automation cabinet for proactive monitoring in ATEX Zone 2*, *MATEC Web of Conferences*, **354**, p. 00044 (2022).
13. S. Paker, I. Ekmekci, *Electrical hazards in industrial facilities and evaluation of the measures*, *Rev. Roum. Sci. Techn.– Électrotechn. Et Énerg.*, **67**, 2, pp. 133-138 (2022).
14. I. C. Mustaţă, L. Bacali, M. Bucur, R. M. Ciuceanu, A. Ioanid, A. Ştefan, *The evolution of Industry 4.0 and its potential impact on industrial engineering and management education*, *Rev. Roum. Sci. Techn.– Électrotechn. Et Énerg.*, **67**, 1, pp. 73-78 (2022).
15. A. Fujiwara, N. Sakurai, *Experimental analysis of screw compressor noise and vibration*, in *International Compressor Engineering Conference*, Purdue (1986).
16. D. Hübel, P. Žitek, *Screw compressor analysis from a vibration point-of-view*, *36th Meeting of Departments of Fluid Mechanics and Thermodynamics AIP Conference Proceedings*, **1889**, p. 020011 (2017).
17. Y. Zhao, J. Feng, B. Zhao, S. Zhou, Z. Tang, X. Peng, *Vibration analysis and control of a screw compressor outlet piping system*, *Proceedings of the Institution of Mechanical Engineers, Part E: Journal of Process Mechanical Engineering*, **233**, 2, pp. 403-411 (2018).
18. M. Cerpinska, M. Irbe, R. Elmanis-Helmanis, *Vibration of foundation for rotary screw compressors installed on skid mounting*, *Engineering for Rural Development* (2018).
19. Y. Wu, V. Tran, *Dynamic response prediction of a twin-screw compressor with gas-induced cyclic loads based on multi-body dynamics*, *International Journal of Refrigeration*, **65**, pp. 111-128 (2016).
20. Y. Kheng, *Why is there water in my air compressor? – Mc-Cast Engineering*, *Mc-Cast Engineering* (2021). <https://mccastengineering.com/reports-blog-en/2019/11/27/why-is-there-water-in-my-air-compressor>.
21. T. Bruce, *Screw compressors: a comparison of applications and features to conventional types of machines*, *Toromont Process Systems*, Sage Energy Corp., Canada (2001).
22. *Screw Compressor Testing*, <https://www.inspection-for-industry.com/screw-compressor-testing.html>.
23. D. Smith, *Pulsation, Vibration, and noise issues with wet and dry screw compressors*, in *Proceedings of the Fortieth Turbomachinery Symposium* September, Houston, Texas, pp. 170-202 (2011).
24. F. Ciuprina, L. Andrei, *Water and thermal aging influence on dielectric response of low-density polyethylene-Al₂O₃ nanocomposites*, *Rev. Roum. Sci. Techn. – Électrotechn. Et Énerg.*, **64**, 4, pp. 303-307 (2019).
25. C. Borzea, A. Morega, D. Comeagă, Y. Veli, *temperature influences on the performances of a PZT-5H piezoelectric harvester*, *12th International Symposium on Advanced Topics in Electrical Engineering (ATEE 2021)*, Bucharest, 25-27 March 2021.
26. C. Săvescu, D. Comeagă, A. Morega, Y. Veli, *Experimental tests with piezoelectric harvester for tuning resonant frequency to vibrating source*, *Rev. Roum. Sci. Techn. – Électrotechn. Et Énerg.*, **67**, 4, pp. 457-460 (2022).
27. A. Ounissi, A. Kaddouri, M. Aggoun, R. Abdessemed, *Second order sliding mode controllers of micropositioning stage piezoelectric actuator with Colman-Hodgdon model parameters*, *Rev. Roum. Sci. Techn.– Électrotechn. Et Énerg.*, **67**, 1, pp. 41-46 (2022).
28. *Midé Technology*, *PPA PRODUCTS Datasheet & User Manual* (2017), <https://cdn2.hubspot.net/hubfs/3841176/Data-Sheets/ppa-piezo-product-datasheet.pdf>.
29. S.A. Kouritem, M.A. Al-Moghazy, M. Noori, W.A. Altabay, *Mass tuning technique for a broadband piezoelectric energy harvester array*, *Mechanical Systems and Signal Processing*, **181**, p. 109500 (2022).
30. C. Borzea, D. Comeagă, *Adjusting the resonant frequency of a cantilever piezoelectric harvester*, *Scientific J. TURBO*, **V**, 2, pp. 11-18 (2018).
31. C. Borzea, C. Comeagă, A. Săvescu, *Boosting the electric response of a cantilevered piezoelectric harvester by constraining tip curvature*, *8th European Conference on Renewable Energy Systems (ECRES 2020)*, Istanbul, Turkey, pp. 344-350, 24-25 August 2020.
32. P. Pillatsch, N. Shashoua, A.S. Holmes, E.M. Yeatman, P.K. Wright, *Degradation of piezoelectric materials for energy harvesting applications*, *Journal of Physics: Conference Series*, **557**, p. 012129 (2014).
33. T.H. Van, T.L. Van, T. Thi, M. Duong, G. Sava, *Improving the output of dc-dc converter by phase shift full bridge applied to renewable energy*, *Rev. Roum. Sci. Techn.– Électrotechn. Et Énerg.*, **66**, 3, pp. 175-180 (2021).
34. A. Subramanian, J. Raman, N. Pachaiyannan, *An efficient hybrid converter for dc-based renewable energy nanogrid systems*, *Rev. Roum. Sci. Techn. – Électrotechn. Et Énerg.*, **66**, 4, pp. 225-230 (2021).